Human Mars Lander Design for NASA's Evolvable Mars Campaign

Tara Polsgrove, Jack Chapman, Steve Sutherlin, Brian Taylor
NASA
Marshall Space Flight Center
Huntsville, AL 35812
Tara.Polsgrove@.nasa.gov

Leo Fabisinski
ISSI – Jacobs ESSSA Group
Huntsville, AL 35812

Tim Collins, Alicia Dwyer Cianciolo, Jamshid Samareh
NASA
Langley Research Center
Hampton, VA 23681

Ed Robertson, Bill Studak, Sharada Vitalpur
NASA
Johnson Space Center
2101 NASA Parkway
Houston, TX 77058

Allan Y. Lee
Jet Propulsion Laboratory
California Institute of Technology
4800 Oak Grove Drive
Pasadena, CA 91109-8099

Glenn Rakow
NASA
Goddard Space Flight Center
8800 Greenbelt Rd
Greenbelt, MD 20771

***Abstract*— Landing humans on Mars will require entry, descent, and landing capability beyond the current state of the art. Nearly twenty times more delivered payload and an order of magnitude improvement in precision landing capability will be necessary. To better assess entry, descent, and landing technology options and sensitivities to future human mission design variations, a series of design studies on human-class Mars landers has been initiated. This paper describes the results of the first design study in the series of studies to be completed in 2016 and includes configuration, trajectory and subsystem design details for a lander with Hypersonic Inflatable Aerodynamic Decelerator (HIAD) entry technology. Future design activities in this series will focus on other entry technology options.**

TABLE OF CONTENTS

1. INTRODUCTION

The human Mars lander will be an essential element of any future human missions to the Martian surface. NASA is currently studying options for sending humans to Mars in the decade of the 2030's. The Evolvable Mars Campaign (EMC) is focused on evaluating architectural trade options to define the capabilities and elements needed for a sustainable human presence on the surface of Mars. [1] The EMC study teams have considered a variety of in-space propulsion options and surface mission options. In each potential scenario a lander capable of delivering between 18 and 27 t of payload to the surface is required. [2] The largest payload landed on Mars to date is the Mars Science Laboratory's Curiosity rover, with a mass of approximately 900 kg. Landing the much larger payloads required for supporting human missions will require alternate approaches.

Because a Mars lander of this scale is significantly outside of our range of experience, mass estimating relationships based on previous lunar and Mars landers could result in large errors in this application. To improve our ability to estimate lander masses for human Mars architecture trades, and to assess other configuration-dependent sensitivities, a more detailed design study is needed. There are several potential entry systems that could support human surface missions including Hypersonic Inflatable Aerodynamic Decelerator (HIAD), Adaptable Deployable Entry and Placement Technology (ADEPT), and rigid aeroshell options with low to mid lift-to-drag ratios (0.2 - 1). All are paired with supersonic retropropulsion (SRP) for descent and landing. Each entry system option will affect the lander configuration and design differently. To assess these technology options and improve our ability to estimate masses a series of design studies has been initiated. The first design study focused on a lander with a HIAD entry system and SRP capable of delivering 27 t of payload to the Martian surface. The results of that activity are presented in this paper and include an overview of the mission, operational requirements, trajectory design, vehicle configuration, subsystem designs, and finally vehicle mass summary and conclusions. Future design studies in this series, expected to conclude in 2016, will focus on landers with other entry technology options.

2. BACKGROUND

The Mars lander consists of three primary elements: (1) the entry system, (2) the Mars Descent Module (MDM), and (3) the payload or cargo. Cargo for a surface mission would include a Mars Ascent Vehicle (MAV) to return the crew to orbit once the mission is complete, and other systems to support surface operations, such as a habitat, mobility systems, power generation systems, in-situ propellant

production plant, science equipment, crew consumables, and spares. These cargo elements would be grouped and delivered using multiple landings. One of the architecture trades under study in the EMC is the cargo capacity of each lander. Minimizing cargo capability per lander would minimize lander size and performance requirements, but require a greater quantity of landers to deliver the needed surface equipment and would make surface operations more complex as assets are utilized from a greater number of landing sites. Examples of cargo packaging options are given in figure 1.

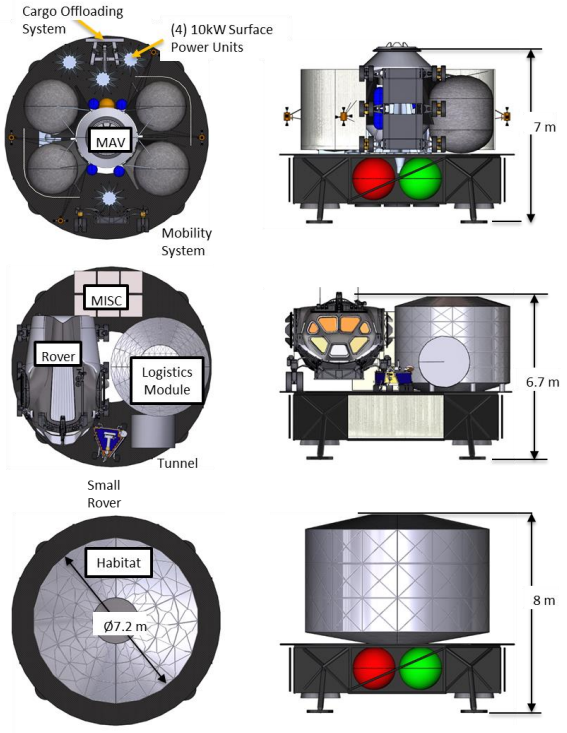

Figure 1 Lander cargo packaging options

Mars landers capable of delivering 18, 27 and 40 t payloads have been studied. The smallest size reasonably capable of supporting human missions is determined by the MAV. The assumption that the MAV cannot be assembled on the surface of Mars makes it the single largest indivisible payload. The MAV assumed uses liquid oxygen (LOX) propellant and methane oxidizer. To minimize launch mass, the MAV is launched without LOX and with a In-Situ Propellant Production (ISPP) plant to make LOX from the Mars atmosphere. Including the structure to support these components the minimum payload mass is 18 t assuming the MAV can carry a crew of four to a 1 Sol orbit (250 x 33,800 km orbit). Five landings would be required to support the first long duration surface mission (500 Sols) using the 18t payload class lander. Landers capable of delivering 27 and 40 t of payload mass have also been studied and those options require 3 and 2 landers respectively for the same mission. [2] At 40 t payload capacity per lander, packaging of cargo elements can become a challenge because many surface cargo elements are pressurized volumes with relatively low density. For this design activity 27 t payload capacity was assumed.

3. Mission Overview

Lander design is influenced by each flight phase from launch through transit, landing and surface operations. In this section the mission phases are described and lander configuration for each mission phase is presented showing the MAV cargo element as an example.

Launch and Transit to Mars

For missions in the 2030's, an evolved Block 2 configuration Space Launch System (SLS) launch vehicle with a 10-meter payload fairing is assumed. There are multiple transportation scenarios under consideration for the EMC involving different in-space propulsion systems and delivery orbits at Mars. See reference 3 for more information on transportation system options. This design study assumes the lander is launched into an elliptical Earth orbit with a Solar Electric Propulsion (SEP) stage that will transport the lander to Mars. Figure 2 depicts the lander as it might appear in launch configuration. There is a conical launch vehicle adapter (LVA) with the SEP stage suspended below. The SEP stage initiates a spiraling Earth escape trajectory with a lunar gravity assist for the final Earth departure. Launch to Earth departure may take 2.5 years using a 300 kW SEP system.

Once Earth escape is achieved, transit to Mars could take another 1.2 years. During Earth escape and transit to Mars it is assumed that the SEP stage will provide power for the lander and its cargo. See figure 3 for Earth to Mars transit configuration.

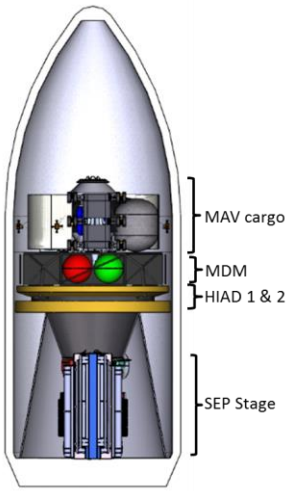

Figure 2. Launch Configuration

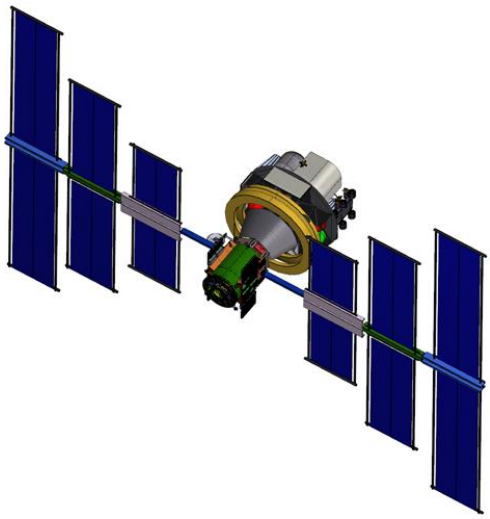

Figure 3. Earth to Mars Transit Configuration

Mars Arrival

At Mars arrival the SEP stage would be jettisoned, and the lander would perform aerocapture to achieve Mars orbit. For this study a 250 x 33,800 km orbit is assumed. This is referred to as a 1 sol orbit because it has an orbital period of one sol, or Martian day (24 h 40 min).

The SEP stage would target the lander for a 40 km minimum Mars altitude pass and then separate from the lander approximately two days prior to Mars atmospheric interface. After separation and through aerocapture the lander would generate its own power using solid oxide fuel cells that pull reactants from the liquid oxygen and methane main propellant tanks. The HIAD (18.8 m diameter) would be deployed some designated time prior to atmospheric interface. See figure 4 for configuration with aerocapture HIAD deployed. The deceleration through the atmosphere would last approximately 7 minutes and result in an orbit with an apoapse of 33,800 km. At apoapse the lander would fire the reaction control system (RCS) propulsion to impart a change in velocity of 15 m/s to raise periapse to a safe distance above the Martian atmosphere, approximately 250 km altitude above the mean areoid. While this lander would be capable of loitering in Mars orbit for 1 year, cargo landers could proceed to the surface soon after aerocapture is achieved. A minimum of 2 Sols of loiter are assumed to allow for state vector updates and proper phasing of the orbit with the landing site. Landers delivering crew to the surface may have to loiter in orbit for several months. The pre-deployed crew lander would remain in Mars orbit until the crew arrive and perform successful docking and transfer of equipment. During Mars orbit loiter the lander would deploy solar arrays to provide power. To mitigate the risk of relying on the same inflatable system after long duration loiter in Mars orbit, a second HIAD is used for entry, descent and landing (EDL). See figure 5 for one possible Mars orbit loiter configuration. In this image the aerocapture HIAD is retained during loiter and would be jettisoned prior to initiation of entry descent and landing. Alternately, it could be jettisoned soon after aerocapture. Retaining it may provide some protection to the EDL HIAD, MDM and cargo from micrometeoroids and orbital debris, but may interfere with solar array articulation. Retraction of the inflatable portion of the aerocapture HIAD may eliminate interference. Further study of the risks associated with Mars orbit loiter is needed to determine a preferred approach.

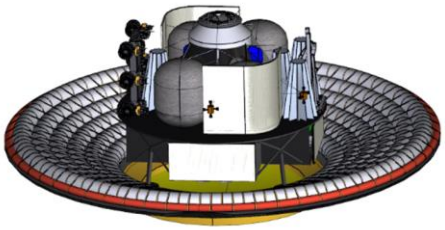

Figure 4. Mars Arrival Configuration

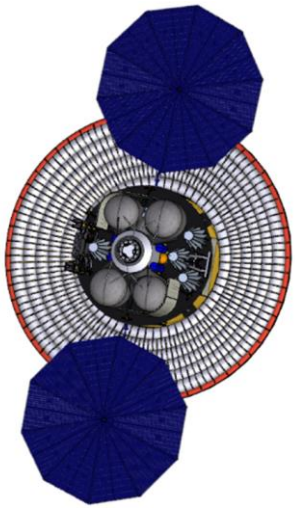

Figure 5. Mars Orbit Loiter Configuration

Mars Entry Descent and Landing

Descent is initiated from apoapsis of the one sol orbit using a 15 m/s RCS burn. The second HIAD (16.7 m diameter) is inflated and entry begins at approximately 125 km altitude. The vehicle flies with a maximum hypersonic continuum lift-to-drag ratio of 0.2 and an angle of attack of -16 deg. The guided entry uses a direct force numerical predictor corrector guidance algorithm to control the vehicle until engine ignition. Initial assessments of flow impingement on payloads during EDL indicates that thermal protection may only be required on the tallest portions of some payloads.

The entry trajectory is designed to maintain maximum deceleration limits below 4 g's for deconditioned crew according to NASA's Human System Integration Requirements. Crew and cargo missions are designed using the same EDL sequence so that pre-deployment of surface

cargo demonstrates the sequence prior to crew arrival. The guidance is targeting the time and location to turn on the engines such that the vehicle can land at an altitude of 0 km above the Mars Orbiter Laser Altimeter areoid. The descent sequence initiates when plugs or doors in the rigid nose heatshield covering the eight 100 kN engines are blown off or opened prior to engine ignition. Additional openings are revealed when the vehicle velocity becomes subsonic to deploy the landing legs. The vehicle retains the HIAD to landing to minimize the risk associated with separation and protect the payload from surface plume interactions. At 12 to 20 m above the surface the engine thrust is reduced such that the vehicle maintains a constant 2.5 m/s until touching down on the surface. Figure 6 illustrates the concept of operations for the reference EDL sequence. As the vehicle nears the surface, the engine plumes will disturb regolith which has the potential to damage the vehicle and other assets nearby. To protect surface assets, landings must occur outside of a predefined keep out zone, currently assumed to be 1 km from any surface asset. Advances in landing accuracy will help to minimize the actual separation distance between landings to no greater than the defined keep out zone. Landing within 100 meters of the landing target is the capability assumed for this mission.

Figure 6. Entry Descent and Landing Operations.

Surface Operations

Once on the surface the inflatable portion of the HIAD would need to be deflated and retracted to allow access to the vehicle. Each lander will have to sustain itself and its cargo for up to 24 hours before surface power assets can be connected to provide power. The surface power system will be among the first cargo elements delivered in any mission scenario. It may take up to 24 hours to deploy and initiate power generation. For subsequent landers it is assumed that a rover would approach the lander and connect a power cable from the surface power infrastructure within 24 hours of each landing. Once surface power is connected, high power payloads such as Liquid Oxygen In-Situ Propellant Production (ISPP) can begin operations.

Lander configuration on the surface must facilitate cargo offloading, crew access, and radiator deployment. ISPP and MAV cargo elements may require significant radiator area that must be deployed once on the Martian surface. Radiator area is dependent upon ISPP production rates and technology assumptions. Crew access to the MAV may require close approach of a pressurized rover with inflatable tunnel. Figures 7 and 8 depict crew access and surface radiator deployment.

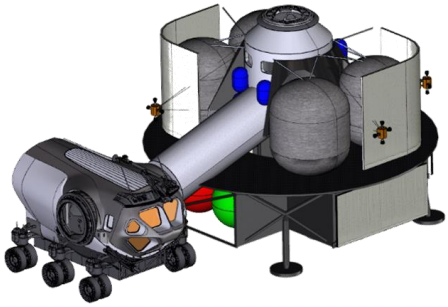

Figure 7. Crew Access Configuration

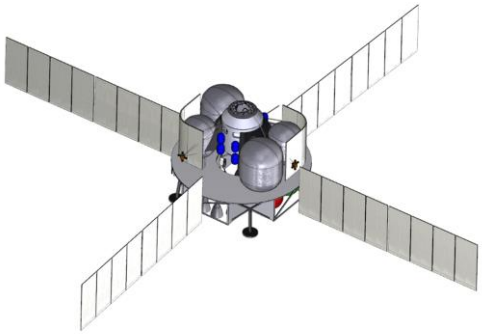

Figure 8. Potential Radiator Deployment to Support Cargo Heat Rejection During Surface Operations.

4. VEHICLE DESIGN

Vehicle subsystems are described in this section followed by a mass summary. Preliminary sizing of an ISPP plant is presented.

Power System

The MDM power system consists of 2 distinct power conversion subsystems feeding a common power management and distribution subsystem. As the lander approaches Mars, it separates from the SEP vehicle and switches its power to its on-board fuel cell power plants. These power plants, known as Solid Oxide Fuel Cells, produce power by reacting Methane and LOX scavenged from the descent fuel tanks. They will power the lander

through Mars Orbit Insertion. During the long Mars orbit loiter, a pair of UltraFlex solar arrays will provide power. These arrays will be discarded immediately before descent to the Mars surface. During descent, and afterward on the surface, the fuel cell power plants will again be used as the power source. They must provide power during the 12 hour descent and the first 24 hours on the surface until the surface power system can be deployed or connected. The power management and distribution system consists of redundant Integrated Power Electronics (IPE) enclosures containing power electronics for array regulation, power conditioning, battery charge control, voltage conversion and switching. The schematic below illustrates the configuration of the Power System

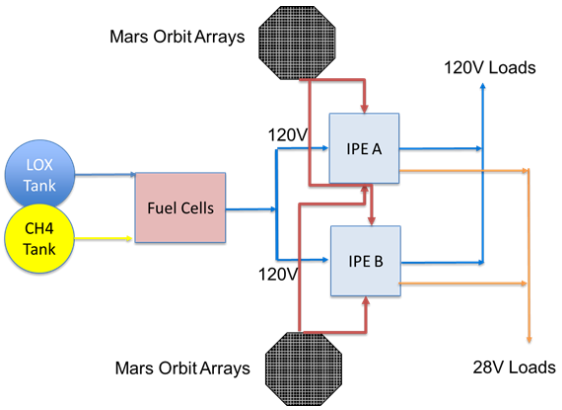

Figure 9. Lander Power System Schematic.

Thermal Control System

The MAV Thermal Control Subsystem (TCS) is fully integrated with the MDM TCS, and the two operate as one subsystem throughout the outbound flight to Mars and on the surface until Mars launch and ascent (when the MAV flies independently). The TCS performs three main functions: (1) mitigate heat loads and losses due to spacecraft interaction with the environment; (2) provide heat rejection for MAV subsystems such as Avionics, Power, ECLS, Human Factors (including crew metabolic heat), and Thermal Control; and (3) provide propellant conditioning for the MAV propulsion system during flight and surface storage. The MAV benefits from the afforded cooling and heat rejection load-sharing across the wide range of thermal environments, especially in the Mars surface environment. This approach also allows for the MAV to carry a minimum amount of TCS subsystem hardware, with the majority being left behind on the MDM at Mars launch. The TCS must operate in a wide range of thermal conditions, such as the diurnal Mars surface environment with its warm and cold extremes, the fairly benign Earth elliptical orbit, and the rather cold Mars orbit/transit environments. The subsystem is composed of insulation systems, heaters and thermal coatings to control temperatures and moderate heat transfer rates to and from the environment. Fluid systems are included, such as pumped coolant loops and cryocoolers with broad area cooling tube networks to perform heat collection and loop heat pipe radiators to reject heat to the environment. Cryocooler and loop heat pipe technologies are currently not at a mature state of readiness. Fault tolerance for TCS elements is provided at the component level for such things as rotating equipment, valves and sensors. A notional subsystem schematic is provided in Figure 10.

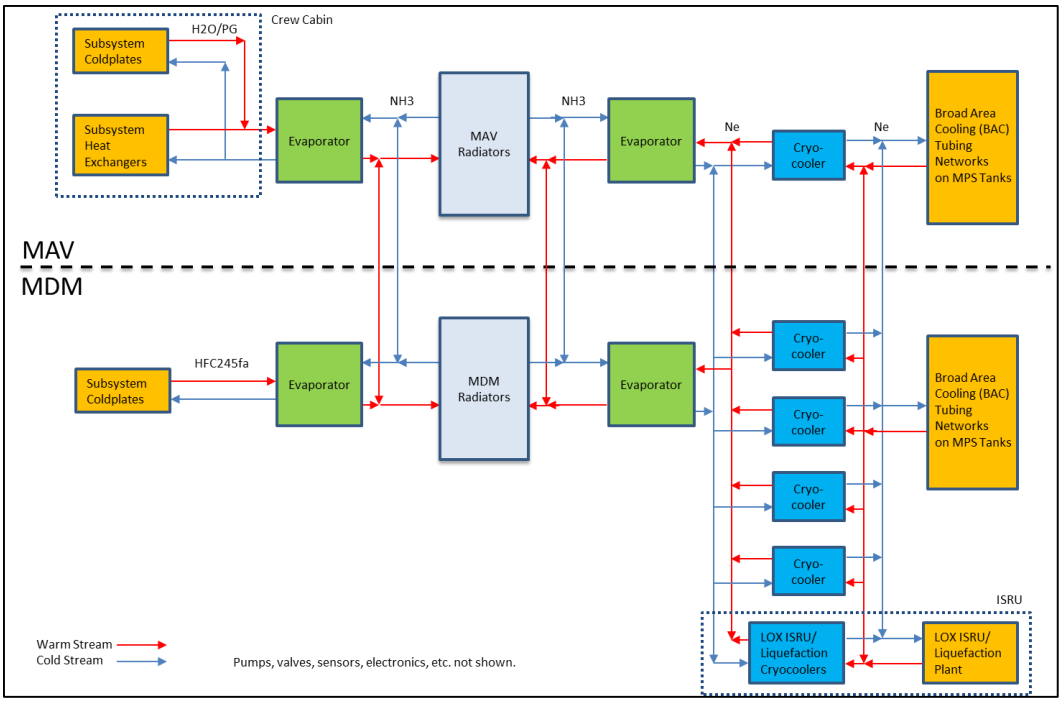

Figure 10. Thermal system schematic.

In-Situ Propellant Production

The ISPP plant is a cargo element that is delivered with the MAV. To determine interface requirements a preliminary design of the ISPP plant was performed. This cargo element affects lander surface configuration due to its significant heat rejection requirements. There are numerous options for each of the steps in oxygen production, liquefaction and transfer to the MAV. In order to provide reasonably high confidence levels for mass, power and performance estimates, a particular combination of technical solutions was chosen based on the maturity of the concepts. For the purposes of this study, the baseline system is located entirely on the MDM and is composed of a Mars atmospheric processing unit which provides dry gaseous oxygen to a liquefaction/accumulator unit, and a pump to transfer liquid up to the MAV propellant tanks. See figure 11. This combination is not necessarily optimal for either the subsystems or the vehicle; forward work will examine the integrated impact of alternative solutions. In this study, the fundamental requirement was to produce approximately 19 t of LOX in less than 10 months; this corresponds to a continuous production rate of 3 kg/h.

The process begins in the ISRU plant, which uses an electrostatic precipitator to provide particle-free gas to the freezer module that captures carbon dioxide (CO_2) while rejecting argon and nitrogen. Periodically, the CO2 is sublimated and sent to a Solid Oxide Electrolyzer (SOE) where the CO2 is converted to oxygen (O_2) and carbon monoxide (CO). The dry gaseous oxygen is then passed to a small accumulator tank and liquefied for temporary storage. A small pump periodically transfers liquid up to the MAV LOX tanks; a return ullage gas line connects the top of the MAV tank back to the liquefaction unit to provide a zero-boil-off closed system. The liquid supply and gas return lines each include a quick disconnect for MAV separation at launch, and each MAV LOX tank has an isolation valve on both liquid and gas lines.

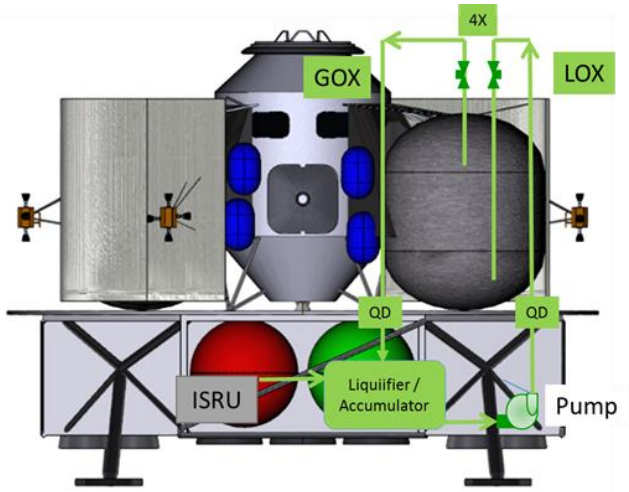

Figure 11. ISRU plant connectivity to MAV

The system mass and power estimates were generated based on a production module size of 1 kg/h. This module size was chosen because it could be used on a precursor mission as a relevant scale production plant, and multiple modules can provide the required flow rate with one spare unit. Thus, 3 units run for production, but 4 units are carried for fault tolerance. The total power required for the ISRU plant is estimated at 26.6 kW, for both plant operation and oxygen liquefaction. Heat rejection for operation and liquefaction is estimated at 17.7 kW. See Table 1. Operation includes: 11.5 kW of power for freezing via cryocooler, 10.2 kW for the SOE, and 0.8 kW for the balance of the plant. Heat rejection of 13.3 kW is required for plant operation. The liquefaction equipment, sized for 3 kg/h, includes a spare cryocooler and transfer pump, but not a spare accumulator tank. Power for the liquefaction unit is estimated as follows: 325W is the required liquefaction cooling capacity, with 25% margin and assuming 10% efficiency for the cryocooler then 4 kW electric plus 4.4 kW thermal rejection. The extensive use of inherently low efficiency cryocoolers for all cooling needs drives both electric power and thermal rejection loads to other subsystems.

Table 1. ISRU Plant Options

		Case 1	Case 2	Case 3
Production Rate	*kg/hr*	1	2	3
Mass	*kg*	333	889	1210
Mass with 25%	*kg*	416	1111	1512
Power	*kWe*	9	17.9	26.6
Thermal Rejection	*kW*	6.1	12	17.7
Approx. HX Area	m^2	114	225	335
Approx. HX Mass	*kg*	287	566	843
Approx. Time to Fill	*months*	26	13	8.7
Number of Units		single unit	2 plus spare	3 plus spare

Some transfer options for forward work include steady liquid transfer to the MAV (i.e. eliminate the accumulator tank) and steady gas transfer to the MAV (i.e. add the liquefaction function to the MAV tanks). Liquefaction may be improved by using compression/heat rejection/throttled expansion (e.g., Linde cycle) along with cryocoolers (sharing the load between the two systems). Functions and equipment could be consolidated, along with the addition of recuperators, load sharing and integrated thermal management. Tailoring production rates for day and night operations may result in reduced radiator area as higher production rates may be possible during cold Martian nights allowing a reduction in the production rate during the warm days while maintaining the desired average production rate.

Command & Data Handling

A single fault tolerant avionics system is assumed. It is also assumed that the avionics system is cross-strapped, which may allow normal operation for more than one fault in the

system when the second fault is not the redundant function of the first failure. In some narrow cases where dissimilar redundancy is possible, more than one fault within the same functional area is possible (e.g., star tracker and inertial measurement unit for rate.)

A safety critical architecture has been assumed. For the command and data handling portion of the avionics, a byzantine resilient computing architecture is used for the critical phases of the mission, e.g., orbit insertion, descend and landing. This is necessary so that the system can "fly-through" a failure and prevent loss of mission. This system can handle any random fault in the system and operate normally (fail operate).

Byzantine resilience is achieved by using a group of four computers (three required, forth increases reliability and allows symmetry in the isolation of units in the architecture). The architecture is designed to use generic single board computers that may be from different vendors (to protect against common mode failures). The underlying technologies to enable the voting byzantine resilience are the time-triggered data bus for the command and control, and the time space partitioned operating system to protect software tasks from crashing the entire system. The data bus physical layer uses the Mil-Std 1553 physical layer (long stub) physical layer but with a new transceiver that runs at 5 MHz instead of 1 MHz. Figure 12 indicates the connections of the various avionics by subsystem to the time-triggered data bus.

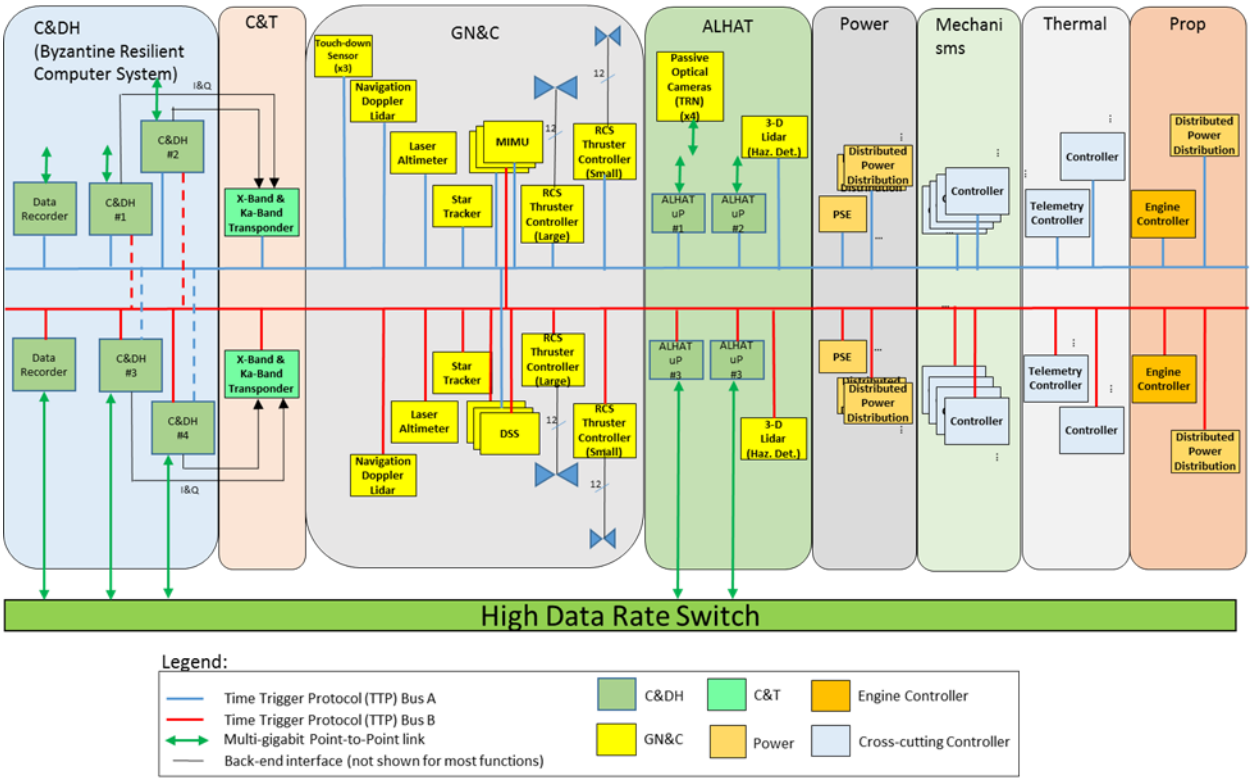

Figure 12. Avionics Network Diagram

Communications and Tracking

Capitalizing on previous architectures and analysis, the communication system for the Human Lander EDL design uses the Deep Space Network to communicate directly to Earth. A robust reliable link at X-band is used for command and telemetry exchange and a Ka-band link is used to return higher rate data to Earth. The data rate on the X-band link is ~7 bps and the downlink data rate on the Ka-band link is ~35 kbps. The notional design of the X-band system includes a deep space X-band transponder (similar to General Dynamics SDST), and solid state power amplifier and patch antenna. This system weighs approximately 9 kg and consumes about 100 W. The Ka-band system includes a Ka-band transmitter, a TWTA and a deployable high gain antenna. This system weighs approximately 62 kg and consumes 185 W.

For this iteration of the communication system design, a DTE link from the Lander to Earth from the surface of Mars was assumed. In future iterations, Mars relays will be considered which would increase the data rates. The feasibility of using an optical communication system will be assessed which would greatly increase the data rates as well as the efficiency of the system.

Once on the Mars surface, communications between the lander, rovers and other assets will be required. The capabilities needed (point to point vs. mesh, tracking, etc,)

and the different standards and protocols that could be adapted to serve this function are still being evaluated.

Guidance, Navigation and Control

Key functions performed by the Guidance, Navigation, and Control (GN&C) subsystem of the Mars lander include the estimation and control of the vehicle's inertial attitude, estimation of the vehicle's state vector (position and velocity vectors), support the pointing needs of the vehicle communication, power generation, and thermal control system, design and execution of trajectory correction maneuvers for flight path control, support the attitude control needs during aero entry, powered descent and landing phases of the mission, and to land safely within 100 m of the pre-selected site on Mars. To perform these functions, a set of placeholder GN&C sensors is selected. It includes an inertial measurement unit and its backup (each with four 1-degree of freedom (DOF) gyroscopes and four 1-DOF accelerometers), a 3-DOF star tracker and its backup, a 2-DOF Sun sensor assembly and its backups, and touch-down sensors for the landing gear.

To meet the entry guidance requirements, a direct force numerical predictor corrector algorithm commands factors that directly control lift and side force (such as vertical and lateral cg movements or flap deflection). This application allows the vehicle to fly at any lift to drag ratio between -0.2 and +0.2 to control the down range distance, and the lateral direct force removes any crossrange component. This strategy eliminates all the open-loop bank maneuvers. A similar approach is used for aerocapture and has been tested in high fidelity simulation and Monte Carlo simulations.

To meet landing safety and accuracy requirements, a placeholder set of ALHAT (Autonomous Precision Landing and Hazard Avoidance Technology) sensors has also been selected. Global precision is enabled with Terrain Relative Navigation (TRN) that provides global navigation by matching real-time terrain sensing data with a priori reconnaissance data stored onboard the spacecraft. Selected TRN sensors include both a passive optical camera and an active lidar unit. Local precision for soft landing is enabled with direct ground-relative velocity measurements. The ALHAT system will use a navigational Doppler lidar to provide high-precision, line-of-sight velocity measurements that enable the GN&C system to control the vehicle's ground-relative velocity during terminal descent to ensure a soft landing. Safe landing is enabled with a lidar-based hazard detection system. It will provide real-time assessment of terrain hazards (craters, slopes, etc.) and the identification of safe landing site(s). The ALHAT system is fully redundant.

Two sets of placeholder thrusters will be used by the GN&C system. Twelve 445-N (100 lbf) thrusters will be used to slew the vehicle in response to pointing commands, to perform orbit maintenance burns, and to provide rate damping about both the pitch and yaw axes during aero entry. Another set of twelve 4,450-N (1,000 lbf) thrusters will be used during the powered descent and landing phase when eight 100 kN main propulsion system (MPS) engines are fired. Control authority about all axes are adequate if the offset of the vehicle's center of mass is maintained to within several centimeters throughout the powered descent phase. GNC algorithms stored in the flight computers (see the Command and Data Handling section) must be designed taking into consideration the large quantities of sloshing liquids in propellant tanks as well as the possible control-structure interaction generated by the presence of the large HIAD structure. Future GNC work will include the development of the navigation architecture and improvements in the RCS thruster configuration. Additional development and testing of the ALHAT system is desired, in particular testing to assess the impacts MPS engine plumes and Mars dust on the performance of ALHAT sensors. The above described GN&C design will evolve as the requirements and vehicle design mature.

Structures

The MDM design is derived from a combination of considerations related to cargo packaging (including an ascent vehicle), offloading, structural efficiency, landing stability, and integration with an aerodynamic decelerator and solar-electric propulsion (SEP) module within a launch vehicle fairing. Thus, the lander configuration and structure must accommodate a broad range of functional and integration requirements. The lander design features a flat deck that can flexibly carry all envisioned cargo elements without design modifications. Propellant tanks, engines, and landing gear are packaged within the descent stage core structure, and a central opening is possible when needed for efficient packaging of an ascent vehicle with an extended engine assembly. See figure 13.

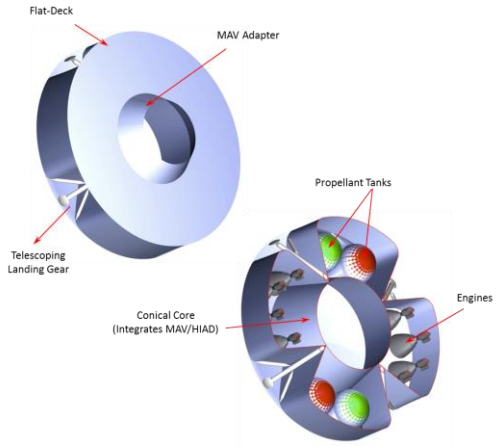

Figure 13. MDM Primary Structure

The MDM structure is shaped to provide efficient load transfer between the cargo elements, a dual HIAD system, and a launch vehicle adapter (LVA) that supports the entire lander stack. For the lander configuration shown in figure 14, the LVA is tall enough to allow an inverted adapter that supports an integrated SEP module. The height of the LVA can be decreased for missions that do not require a SEP

module, without affecting the overall lander design or means of integration with the HIAD.

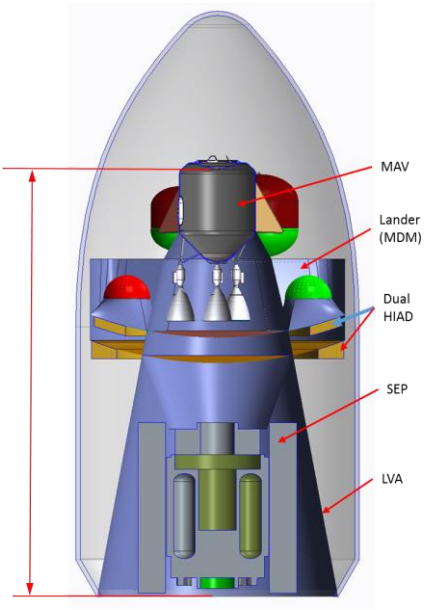

Figure 14. Launch Configuration Primary Structure

Main Propulsion System

The primary purpose of the main propulsion system is to store, maintain and deliver the fluids required by the engines of the lander to operate. The liquid methane and oxidizer are each stored in a pair of tanks and kept at cryogenic temperatures through active and passive thermal management systems. A system of ducts, lines, and valves performs fill and drain functions as well as propellant transfer to the engines via feed lines. Each pair of tanks is linked with a cross over line to maintain equal levels in the tanks and allow for a single fill and drain port for each of the fluids. Prior to engine operation, the tanks are pressurized with high pressure helium gas supplied to the ullage. While the engines are firing, the methane tanks are pressurized autogenously with warm methane gas bled off from the flow in the engine. The oxygen tanks will be pressurized with helium. Currently, the helium is planned to be kept at ambient conditions to simplify the design. A future risk/benefits analysis may warrant changing the design to a cryogenic helium storage system, in which the helium is stored in the oxidizer tank, or an oxygen autogenous pressurization system. The design of one half of the main propulsion system is laid out in the schematic shown in figure 15. The other half is a mirror image of this.

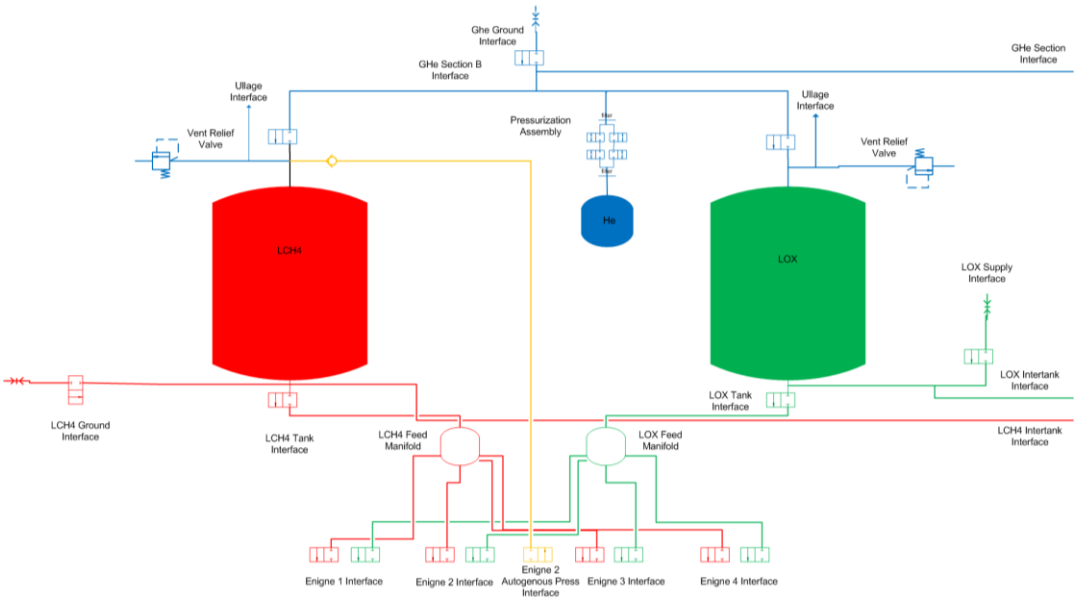

Figure 15. Main Propulsion System Schematic (one half of the complete system depicted here)

The main propulsion system is expected to require approximately 6 kW of electrical power to run the feed system during engine burns and about 1.5 kW intermittent electrical power to run the pressurization system. The expected quantity of propellant required for the decent burn was developed from an integration of the thrust profile with 8 100 kN engines and the mass flow rate as a function of throttle position. Additional considerations for useable propellant such as reserve and RCS and unusable propellant such as residuals, fuel bias, and boil off are accounted for in the propellant inventory.

Main Engine

A gas generator cycle was selected for the baseline engine concept based on a trade study investigating quantitative performance analysis and qualitative discussions on reliability and development risk. The trade space was defined

under the constraints of; minimum thrust of 100 kN, minimum specific impulse (Isp) of 360s, maximum diameter less than 1 m, and a 5:1 throttle capability. Each cycle was constrained to thrust and envelope, while Isp was allowed to vary as a model output. The cycles are compared in figure 16, showing Isp as a function of chamber pressure. Although the expander cycles were shown to meet the Isp requirement, they lack Isp margin. Also, limitations on available power to drive this cycle will limit future growth in total thrust which may be needed if there is mass growth in the vehicle design greater than estimated in this study.

In addition to the performance constraints for EDL, there are programmatic desires for a common engine between the MDM, ascent vehicle, and in-space stages. These desires placed additional emphasis on ignition reliability, design margins, and development risks. Staged combustion cycles were found to have significant performance advantages, but were qualitatively judged to have lower reliability and higher development risk. Ultimately, the gas generator cycle was chosen based on its performance margin relative to the constraints and advantages in terms of ignition processes and development maturity. The baseline engine power balance results in a chamber pressure (Pc) of 1500 psi, Turbine temperature of 1800 R, mixture ratio of 3.2, and a resultant Isp of 368 s. Trajectory design and vehicle propellant loads were calculated assuming a maximum Isp of 360 seconds, with an Isp margin of 8 seconds.

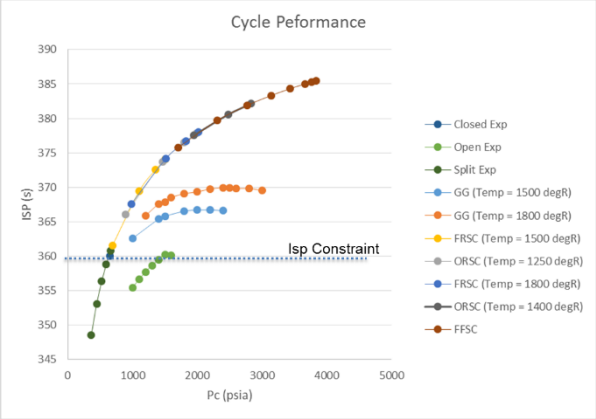

Figure 16. Engine Cycle Performance Trade

Secondary Propulsion

The chemical RCS for the lander is a straight forward pressure-fed propulsion system using liquid oxygen (LOX) and liquid methane (LCH4) stored in the main propellant tanks. For the initial concept design, the attitude control system uses a combination of thrust levels; 110 N – 445 N (25 lbf – 100 lbf) for the in-space orbital phase of flight and 4500 N (1000 lbf) for control during the entry and descent phase of the mission. The system is intended to be single-fault tolerant at the component level (i.e., dual string), and two-fault tolerant at the functional level (i.e., control maneuvers could be accomplished in more than one way in the event of a thruster failure). A full control analysis is still needed to determine the exact thrust level, placement and orientation of the thrusters. The RCS propellants are common to and stored in the main propellant tanks for thermal conditioning during the cruise portion of the mission, but are transferred and pressurized in a set of accumulator tanks in between each mission phase for on-demand usage. The accumulator tanks are sized for EDL, the most demanding phase. The tanks turned out to be surprisingly larger than initial anticipated. Further work is proposed to optimize the control authority, accumulator tank sizes and pressurization pump power allowing for more modest tank sizes with the recharge pump running continuously during more demanding phases of the flight.

Entry System

The entry system design is based on the HIAD ground development projects and the Inflatable Reentry Vehicle Experiment (IRVE) flight demonstrations [Refs. 4-6]. The HIAD model used in this design study consists of an inflatable structure, inflation gas, inflation system, flexible thermal protection system (F-TPS), rigid nose, HIAD attachment ring, center of gravity shift mechanics, and aeroshell instrumentation. See figure 4. The HIAD aeroshell is a 70 degree sphere cone, with the inflatable structure forming the conical section and a rigid nose forming the spherical section. The inflatable structure is a stacked-toroid design with pairing loops and radial straps to tie toroids together and carry radial loads, axial cords to carry the buckling loads, braided fabric to counter the toroid hoop stress, and a thin film gas barrier. The flexible thermal protection system consists of two layers of ceramic outer fabric, several layers of flexible primary insulation (quantity is customized for mission requirements), one layer of flexible secondary insulation, and a gas barrier.

The vehicle uses two HIADs, one that is jettisoned after the aerocapture pass and another deployed just prior to deorbit. HIAD sizing is accomplished using an integrated system analysis model that is made of several parametric models. These models are mathematical representations that predict the component mass from the vehicle dimensions and mission key environmental parameters such as the maximum deceleration and total heat load. Sizing for this application resulted in an aerocapture HIAD of 18.8 m in diameter when inflated and an EDL HIAD of 16.7 m in diameter inflated. The details of an earlier HIAD parametric model implementation can be found in Reference. 7. Continued refinement of the parametric model is planned for 2016.

5. Vehicle Mass Summary

A summary of all vehicle masses is given in Table 2. These masses include mass growth allowance applied in accordance with AIAA standard ANSI/AIAA S-120A-2014 at the component level. No other margins are included in this table, however the application of a program manager's reserve in addition to mass growth allowance is prudent for architecture studies. Total dry mass margin for this system is 4.4 t which

represents and average mass growth allowance of 24% of the dry mass (excluding payload). Subsystems were designed to be single fault tolerant for critical functions. Additional fault tolerance may be required to meet future reliability goals, but further study with detailed reliability analysis would be required to determine the most mass efficient and effective application of additional redundancy.

Table 2. Vehicle Mass Summary

Mass Breakdown Structure			Predicted Mass (kg)
1.0	**Structures**		**4916**
	1.1	MDM Primary Structure	1599
	1.2	MDM Rings/Beams	355
	1.3	MDM Structural Joints and Interfaces	494
	1.4	HIAD Support Structure	847
	1.5	Landing Gear	1620
2.0	**Propulsion**		**5570**
	2.1	Main Propulsion System (MPS)	3933
	2.2	Reaction Control System (RCS)	1636
3.0	**Power**		**1437**
	3.1	Solar Power System	845
	3.2	Fuel Cell Power System	210
	3.3	Power Management and Distribution	382
4.0	**Avionics**		**413**
	4.1	Command & Data Handling	214
	4.2	Communications & Tracking	77
	4.3	Guidance Navigation & Control	122
5.0	**Thermal**		**573**
	5.1	Active cooling loops	200
	5.2	Heaters	13
	5.3	Radiators	360
6.0	**HIAD**		**10689**
	6.1	Aerocapture HIAD	6081
	6.2	EDL HIAD	4608
7.0	**Cargo**		**27000**
	7.1	MAV + MAV-to-MDM Adapter	17334
	7.2	ISRU	1512
	7.3	ISRU Radiators & Deployment Mechanisms	1130
	7.4	Other Cargo	7024
		Dry Mass	**50597**
8.0	**Non-Propellant Fluids**		**971**
	8.1	Thermal Control	63
	8.2	Fuel Cell Reactants	279
	8.3	Propellant Residuals, Reserves, Fuel Bias, Boil off	629
	8.4	Propellant Pressurization	16
		Inert Mass	**51568**
9.0	**Propellant**		**13774**
	9.1	MPS Propellant	9067
	9.2	RCS Propellant	4706
Total Mass			**65341**

6. CONCLUSIONS

A preliminary design of a human Mars lander using a HIAD entry system has been presented. The analysis conducted includes development of an initial configuration and cargo packaging assessments, EDL trajectory optimization, evaluation of flow impingement on payloads, and preliminary design of all vehicle subsystems. Additionally, preliminary design for the ISPP cargo was performed to determine interface requirements. This design is capable of delivering 27 t of payload to the Martian surface. The next steps will be to evaluate changes in the design for 20 t of payload capability. This design and the 20 t payload capability variant will further improve the basis for parametric vehicle sizing model development which will enable more rapid evaluation of trade space alternatives. Forward work on this concept will be primarily focused on continued development of parametric models for vehicle sizing and improving the EDL trajectory simulation capability. Alternative entry system technologies will also be studied.

ACKNOWLEDGEMENTS

The authors acknowledge the contributions of the late Dr. Kendall Brown who led human Mars lander design studies in the years preceding this work and upon whose work the initial design was based. The authors thank the Evolvable Mars Campaign leadership for supporting this work and the HIAD Project Team for providing expertise and guidance on HIAD performance and integration issues. The authors recognize design team members Dan Thomas, Mike Baysinger, Dave Paddock, John Teter, D.R. Komar, and Ashley Korzun for their valuable contributions to vehicle integration, configuration, structures and aerodynamics analysis. Part of this research was carried out at the Jet Propulsion Laboratory, California Institute of Technology, under a contract with the National Aeronautics and Space Administration.

REFERENCES

[1] Craig, Douglas A., Troutman, Patrick, Herrmann, Nicole,"Pioneering Space Through and Evolvable Mars Campaign," *AIAA SPACE 2015*, Pasadena, CA, August 31-September 2, 2015

[2] Toups, L., Brown K., and Hoffman, S. J., "Transportation-Driven Mars Surface Operations Supporting an Evolvable Mars Campaign," *IEEE Aerospace Conference* 2015

[3] Percy, T., McGuire, M., Polsgrove, T., "In-space Transportation for NASA's Evolvable Mars Campaign," *AIAA SPACE 2015*, Pasadena, CA, August 31-September 2, 2015

4) Hughes, S. J., Dillman, R. A., Starr, B. R., Stephan, R. A., Lindell, M. C., Player, C. J., and Cheatwood, F. M., "Inflatable Re-entry Vehicle Experiment (IRVE) Design Overview," AIAA Paper AIAA 2005-1636, 18th AIAA Aerodynamic Decelerator Systems Technology Conference and Seminar, Munich, Germany, May 23-26, 2005

5) Hughes, S., Cheatwood, M., Dillman, R., Wright, S., Del Corso, J., Calomino, A., "Hypersonic Inflatable Decelerator Technology Development Overview", AIAA 2011-2524, 21st AIAA Aerodynamic Decelerator Systems Technology Conference and Seminar, 23-26 May 2011, Dublin, Ireland

6) Lichodziejewski, L., Kelley, C., Tutt, B., Jurewicz, D., Brown, G., Gilles, B., Barber, D., Dillman, R., Player, C., "Design and Testing of the Inflatable Aeroshell for the IRVE-3 Flight Experiment", AIAA 2012-1515, 53rd Structural Dynamics and Materials Conference, 23-26 April 2012, Honolulu, Hawaii

7) Samareh, J.A., and Komar, D.R., "Parametric Mass Modeling for Mars Entry, Descent, and Landing System Analysis Study," AIAA-2011-1038, 2011

BIOGRAPHY

Tara Polsgrove *is an aerospace engineer in the Flight Programs and Partnerships Office at NASA's Marshall Space Flight Center. She has been with NASA since 2000 and has worked on many conceptual designs of advanced spacecraft, including performance and vehicle integration for the Altair Lunar Lander. Her background is in interplanetary trajectory optimization and mission analysis. Recent work has focused on Mars transportation and lander designs supporting missions to send humans to Mars. Ms. Polsgrove has a Bachelor of Science in Aerospace Engineering from the Georgia Institute of Technology and a Master of Science in Engineering with a Systems Engineering focus from the University of Alabama in Huntsville.*

Jack Chapman *is a propulsion systems engineer in the Advanced Concepts Office, Engineering Directorate at NASA's Marshall Space Flight Center in Huntsville, Ala. Mr. Chapman has a wide range of propulsion experience, but specializes in the design, development, fabrication and testing of pressure-fed momopropellant and bipropellant chemical propulsion systems. Mr. Chapman has contributed to many preliminary design activities including STS Liquid Flyback Booster, Space Station, and numerous Lunar and Mars robotic landers, rovers, and sample return designs. Recently, he was responsible for development of LOx/LCH4 reaction control and main thruster development work and continues to conduct 'green-propellant' propulsion development for nano-satellites applications. He was lead test engineer for the Lunar Atmosphere and Dust Environment Explorer (LADEE) propulsion system launched in 2013. Mr. Chapman received his bachelor's degree in aerospace engineering in 1988 from Auburn University and has studied at the Moscow Aviation Institute. Mr. Chapman joined NASA/MSFC in January 1989*

Steve Sutherlin *is a thermal control engineer in the Advanced Concepts Office at NASA's Marshall Space Flight Center. He is currently responsible for thermal design and analysis pertinent to the Mars Ascent Vehicle (MAV) and related studies. Mr. Sutherlin has 35 years of experience in thermal design, analysis and testing of NASA and DoD space vehicles, payloads and hardware. He received the Bachelor of Chemical Engineering degree from Auburn University.*

Brian Taylor *is an aerospace engineer in the Propulsion Systems Department at NASA's Marshall Space Flight Center. He has been with NASA in the Main Propulsion Systems Branch since 2013. Recent work has included nuclear propulsion technology development and main propulsion system design for liquid rocket engines. He has a background in liquid rocket engines and air breathing propulsion systems as well as plasma and laser physics. Mr. Taylor has a Bachelor of Science in Aerospace Engineering from Missouri University of Science and Technology, a Master of Science in Aerospace Engineering from Pennsylvania State University, and is seeking a PhD in Mechanical Engineering at the University of Alabama in Huntsville*

Leo Fabisinski *is the power systems lead for the Advanced Concepts Office of Marshall Space Flight Center. His responsibilities include conceptual design and sizing of spacecraft power systems, design of advanced power electronics for small spacecraft, and evaluation of emerging power technologies.. He is also a Power Systems Subject Matter Expert (SME) for Propulsion Research and Technology - leading the team currently developing Linear Transformer Driver (LTD) pulsed power technology in the advanced propulsion branch. He is co-inventor of the Lightweight Integrated Solar Array (LISA) and developer of the innovative power regulator for LISA. Mr Fabisinski graduated with a BS from Vanderbilt University in 1978. He has worked as an electronic designer in medical diagnostics, digital audio, and telecommunications fields before coming to Marshall in 2002.*

Tim Collins *is a senior structures research engineer in the Structural Mechanics and Concepts Branch at NASA Langley Research Center in Hampton, Virginia. His area of expertise is spacecraft structural design and analysis with an emphasis on conceptual-design trade studies supported by hardware-prototype demonstrations. He has been with NASA since 1987, working on structural concepts for numerous NASA programs ranging from precision telescopes to Lunar and Mars landers. He also specializes in structurally efficient concepts for robotic operations, including those required for in-space or surface-based servicing and assembly. Mr. Collins has a Bachelor's Degree in Physics from the University of Rochester and a Master of Science Degree in Mechanical and Aerospace Engineering from the University of Virginia.*

Alicia Dwyer Cianciolo *is an aerospace engineer at the NASA Langley Research Center. She specializes in developing simulations to analyze vehicle flight through different atmospheres in the solar system. Primarily focusing on Mars over the past 15 years, she has worked on several missions to the planet including the Odyssey and Reconnaissance Orbiter aerobraking operations, the Exploration Rovers, and as a member of the Entry, Decent and Landing Team that successfully landed the Curiosity Rover on Mars in August of 2012. She is currently supporting NASA's the next lander mission to Mars, InSight, and is working to analyze entry technologies that will enable human exploration of the planet. She holds a Bachelor of Science degree in Physics from Creighton University and a Master of Science degree in Mechanical Engineering from The George Washington University.*

Jamshid Samareh *is a senior research aerospace engineer in the Vehicle Analysis Branch of NASA Langley Research Center. His research interests are in Entry, Descent, and Landing (EDL), mass modeling, multidisciplinary analysis and design optimization (MDAO), fluid-structure interaction, geometry modeling, and shape optimization.*

Bill Studak *is a senior design/analysis/build/test engineer with 23 years of experience in propulsion and fluid systems, components and related flight hardware. He has worked on propulsion systems for the Space Shuttle, Space Station and numerous developmental efforts at NASA's Johnson Space Center. Most recently he has been testing prototype hardware for non-toxic, high performance and space storable propellants suitable for next generation missions to the Moon and Mars. Mr. Studak has authored or coauthored multiple technical reports and papers on green propellant technology development and he has a B.S. degree in Mechanical Engineering from the University of Texas.*

Sharada Vitalpur *is the Deputy Branch Chief and Chief Architect of the Wireless and Space Communication Systems Branch at Johnson Space Center. Her expertise is in communication systems, architecture, signal processing and end-to-end analysis. She has worked on different communication systems for the Space Shuttle, the International Space Station and was the C&T System Manager for Orion. Ms. Vitalpur started her career at ITT Aerospace Corporation designing, analyzing, modeling and implementing algorithms and protocols for different DoD communication systems. She has numerous publications and attended Purdue University in West Lafayette, Indiana where she received her Master of Science in Electrical Engineering and Bachelor of Science in Electrical Engineering with Highest Distinction.*

Allan Y. Lee *is with the Guidance and Control section of Jet Propulsion Laboratory, California Institute of Technology. He received his Ph. D. degree from the Aeronautics and Astronautics department of Stanford University. From 1990 to date, he worked on the design, build, testing, launch, and mission operations of the attitude control system of the Cassini spacecraft, a mission to Saturn and Titan. In 1999-2009, he was the Cassini attitude control operation team leader. In 2007-2010, he was the Guidance, Navigation, and Control subsystem manager of the NASA Altair Human Lunar Lander project. He has been awarded a NASA exceptional service medal and an exceptional achievement medal. Dr. Lee has authored or co-authored 50 journal papers, and two book chapters in Engineering, Technology, and Applied Science Series*

Glen Rakow *is an electronics engineer at NASA/GSFC. He began working at NASA in 1989. Early part of his career focused on designing electronics for 5 small in-house spacecraft, as part of the Small Explorer (SMEX) Project. This work transitioned into designing with FPGAs for SMEX-lite that eventually became TRIANA (1998), a mission that was moth-balled for 12 years and eventually launched as DSCVR by NOAA (2015). In 1998, Mr. Rakow started evaluating and designing to IEEE-1355, which eventually became SpaceWire, the first SpaceWire implementation in the US and flown on Swift (2003). Since 2003, Mr. Rakow has collaborated with ESA for the evolution of SpaceWire to include the protocol ID and several SpaceWire protocols. He has continued to advocate and infuse SpaceWire into many NASA missions, and has overseen the transfer of NASA SpaceWire technology to US industry. In 2007, Mr. Rakow started working on Constellation and was later the Altair Avionics Lead. In this role Mr. Rakow worked to develop safety critical architecture for Altair using modular spacecraft component building blocks (SpaceFRAME), along with time-triggered networks and time-space partitioned software. Also in 2007, Mr. Rakow started representing NASA in the CCSDS Spacecraft Onboard Interface Services work group to define services for onboard spacecraft, this work has transitioned into the definition of electronic data sheets (CCSDS blue book) for spacecraft components specification, and currently process for integrating deterministic networks into spacecraft. Mr. Rakow continues to evaluate and develop spacecraft avionic technologies for NASA crew and robotic missions. He earned a Bachelor of Science in Electrical Engineering from the University of Maryland, Collage Park, in 1988, and a Master of Science in Electrical Engineering from George Washington University, Washington D.C., in 1997.*